Eur. Phys. J. B **48**, 463–468 (2005)
DOI: 10.1140/epjb/e2006-00002-8

THE EUROPEAN PHYSICAL JOURNAL B

Structural characteristics of ultra-low k SiO_2 thin films prepared using a molecular template

Z.-W. He[1], W.-X. Sun[2], X.-Q. Liu[1], D.-Y. Xu[1], J. Gou[1], and Y.-Y. Wang[1,a]

[1] Department of Physics, Lanzhou University, Lanzhou 730000, P.R. China
[2] Physics Staff Room, the Sixth Middle School of Shijiazhuang, Shijiazhuang 050051, P.R. China

Received 15 January 2005 / Received in final form 25 September 2005
Published online 19 January 2006 –

Abstract. Nanoporous SiO_2 thin films with ultra-low dielectric constants were synthesized using a molecular template method. Uniform films with pore size between 10 and 20 nm were obtained as observed by N_2 adsorption/desorption isotherms and transmission electron microscopy. Fourier transform infrared spectroscopy (FTIR) and differential thermal analysis were carried out to investigate the effect of n-hexane washing on structural properties before and after the surface modification process. The results showed that –OH bonds were substituted with $-CH_3$ bonds in the films as a result of modification of trimethylchlorosilane (TMCS)/*n*-hexane solution. Four kinds of model were used to analyze the relationship between porosity and dielectric constant of the films, where the dielectric constant was determined from capacitance-voltage measurements. The investigation indicated that the corresponding relationship was in accord with that estimated by the Rayleigh model.

PACS. 77.55.+f Dielectric thin films

1 Introduction

The basic technological aim in ultra-large scaled integration (ULSI) is the realization of a higher device speed with closer packing density, which results in multilevel interconnection. Interconnection delay, generally termed as resistance-capacitance (RC) time delay, which is mainly dominated by parasitic capacitance, has received much attention over the basic gate delay in deep submicron devices [1]. According to the equation, $RC = 2k\rho\varepsilon_0 L^2(4/p^2 + 1/T^2)$, (where ρ is the resistivity of interconnection, k the relative dielectric constant, and ε_0 the permittivity of vacuum) [2], reducing ρ or k is regarded as an effective way to decrease RC time delay. As a result, Cu has recently been used as a substitute for Al in the interconnected line to reduce the resistance [3]. However, further performance gain is still limited by the intra and interlayer capacitances. This has fueled the frantic search for new dielectrics with lower k value [4–6].

Nanoporous SiO_2 thin films are regarded as one of these optional candidates, with their potential for ultra-low k as well as better thermal and mechanical stability [7]. In particular, the k value of the films is tunable according to porosity, and thus can be tuned to fit existing microelectronics technology [8]. Sol-gel method is one of the suitable techniques to prepare nanoporous SiO_2 films. However, the films derived from this method have some limitations in actual application, i.e., they usually have the problem of hydrophobicity and larger range of pore size distribution, which weaken the electrical and mechanical properties of the films [9]. The phenomenon of hydrophilicity results from a large quantity of Si-OH bonds sticking out from the pore surface, while the formation of pores in the films is based on ethanol volatilization which intricately scatters in sol. Generally, hydrophilicity can be partially controlled through surface modification. Improved control of pore size is achieved through the introduction of templates in the preparation process. Few groups have systematically discussed the structural characteristic of nanoporous SiO_2 films when introducing templates, which was an important foundation for interpretation of the electrical and mechanical properties. In this paper, we report the synthesis and structural properties of nanoporous SiO_2 films with ultra-low k prepared by sol-gel method with polyoxyethylene ether (PEE) as template. The effects of *n*-hexane washing, surface modification and thermal treatment on the structure are discussed in detail.

2 Experimental

The wet gel was synthesized through hydrolysis and condensation of tetraethoxysilane (TEOS) with hydrochloric acid (HCl) as catalyst. Before thin film preparation,

[a] e-mail: wangyy@lzu.edu.cn

TEOS was firstly mixed with ethanol and de-ionized water. 0.1 g of non-ionic surfactant (PEE) was then added to the stock solution and stirred until it dissolved completely. HCl was used as catalyst. By spin coating, the surface of a Si substrate was fully covered with the solution. Both aging and washing processes were conducted in saturated water vapor and in n-hexane solution, respectively. The detailed preparation conditions including spin coating, surface modification, and thermal annealing are described in reference [10].

Fourier transform infrared spectroscopy (FTIR; Nicolet NEXUS 670) was used to compare the changes of the chemical structure with n-hexane washing, surface modification and thermal annealing. Thermo-gravimetric and Differential thermal analysis (TG-DTA; DUPONT 1090B) were performed to examine the compositional change with temperature. The nanometer pore size, and the microstructure of the films were characterized by the N_2 absorption/desorption isotherms, transmission electron microscopy (TEM; JEOL 100CX) and high resolution scanning electron microscopy (HR-SEM; JSM-5600LV), respectively. The relationship between porosity and dielectric constant, k, was described by four models, where the k value was calculated from the refractive index, which was consistent with that determined from the capacitance-voltage ($C-V$) measurements.

3 Results and discussion

Figure 1a is FTIR spectrum of the film modified by pure trimethylchlorosilane (TMCS) but not treated with the n-hexane washing process. When the same film was treated with both washing in n-hexane solution and surface modification in TMCS/n-hexane solution, the resultant of FTIR measurement is shown in Figure 1b. In both spectra the peak at 3650 cm^{-1} corresponds to the non-associated –OH bonds that exist in the surface of the pores in the SiO_2 film. Two absorption peaks in the range of 2930–2970 $cm^{-1}$are associated with the stretching vibrations of the $–CH_3$ bonds. Comparing with Figure 1a, the intensity of the absorption peak of $–CH_3$ in Figure 1b increases significantly, while the intensity of the absorption peak at 3650 cm^{-1} decreases. This indicates that the non-associated –OH bonds are well substituted by $–CH_3$ bonds after the n-hexane washing process. It is clear that surface modification is a kind of chemical reaction, through which the –OH bonds in the pore surface can be substituted with $–CH_3$ bonds. If there are some chemical reactions that occur in the TMCS before surface modification, the corresponding substitution cannot be fully achieved. Theoretically, TMCS can react with water and ethanol, but cannot react with n-hexane, although it has good miscibility with n-hexane [11]. Therefore in the washing process, the replacement of water and ethanol in pores with n-hexane is essential.

Figure 2a is a FTIR spectrum of a nanoporous SiO_2 film with significant surface modification. The film was treated through washing in n-hexane solution, followed by surface modification in TMCS/n-hexane solution, as

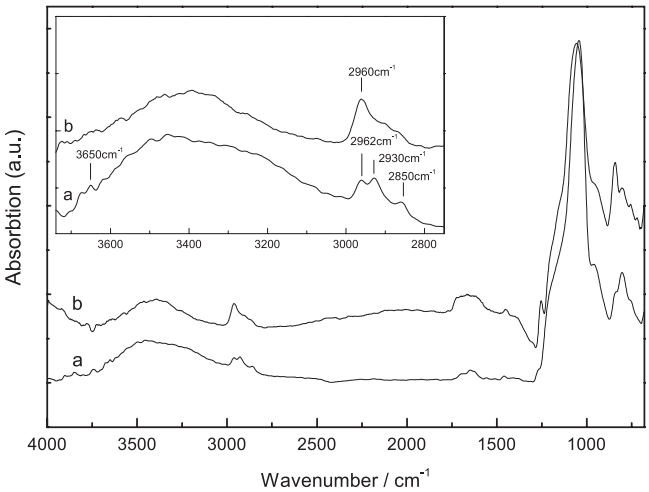

Fig. 1. FTIR spectra of samples that have been surface modified and thermally treated at 200 °C in N_2 atmosphere. (a) modified in pure TMCS; (b) washed by n-hexane and modified in TMCS/n-hexane solution.

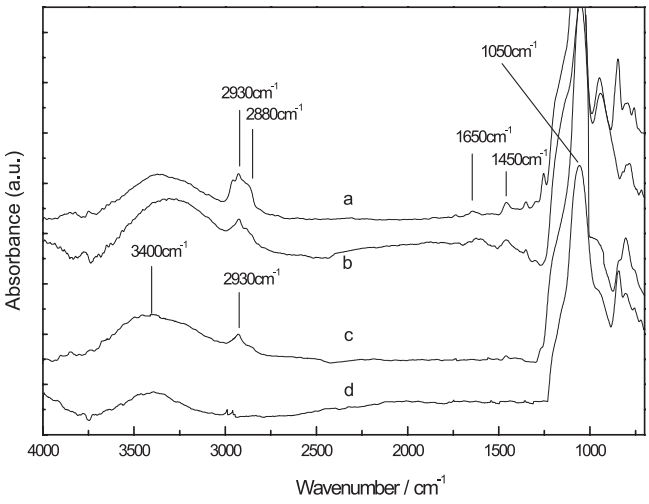

Fig. 2. FTIR spectra of samples modified in TMCS/n-hexane solution (a) no-thermal treatment; (b) thermal treatment at 200 °C in N_2; (c) 450 °C in N_2; (d) 450 °C in air, respectively.

for that of Figure 1b. The most intense absorption peak centered at 1050 $cm^{-1}$is an asymmetric stretching vibration of Si-O-Si bonds. The presence of this peak confirms the formation of a network structure inside the film [12]. A broad absorption peak located at 3400 cm^{-1} was also observed, which corresponds to the associated –OH bond. The peak at 2880 cm^{-1} is attributed to the $–CH_2–$ of the ethoxy group, which is caused by incomplete hydrolysis of the TEOS or re-esterification. The peak at 2930 cm^{-1} originates from a $–CH_3$ stretching vibration, resulting from surface modification in TMCS/n-hexane solution.

When the film was further thermally annealed at 200 °C in a N_2 atmosphere, the chemical bonds were found to have shown some changes. The results are shown in Figure 2b. The absorption peak at 2880 cm^{-1} decreased significantly because of the decomposition of the molecular

template, and pyrolytic loss of organic material in the film. As a result of volatilization of the water adsorbed in the structure, the peak at 3400 cm^{-1} was also found to be greatly reduced. Some small peaks around 1400 cm^{-1} and 1600 cm^{-1}, corresponding to C–H and –OH bonds, respectively, become weaker. On the other hand, the wave number of the most intense absorption peak at 1050 cm^{-1} showed no obvious change. From the relationship [13]: $(\omega^2 = \frac{\alpha}{m_O}(1 - \cos\theta) + \frac{4\alpha}{3m_{Si}}$, where m_o and m_{Si} are the mass of oxygen and silicon atoms, respectively, ω the frequency of absorption, α the vibration constant, and θ the bond angle), we believe that the bond angle of Si-O-Si bonds is thermally stable, and the network structure kept unchanged after thermal treatment at 200 °C in N_2 atmosphere. Figure 2c is the spectrum of the film thermally treated at 450 °C in N_2 atmosphere. The absorption peak at 3400 cm^{-1} decreased significantly, while the $–CH_3$ absorption peak at 2930 cm^{-1} showed a slight decrease. The thermal treatment at higher temperatures caused further pyrolysis of the organic components. However the pyrolysis was confined to a certain extent due to the presence of a N_2 atmosphere. This was confirmed from the comparison with the spectrum of the film thermally treated in air, as shown in Figure 2d, in which the decrease of the $–CH_3$ peak was more obvious than that in Figure 2c.

From the results above, we can see that the uniformity of the microstructure of the films mainly involves two factors. Firstly, molecular templates with uniform distribution in sol are essential. The nanoporous SiO_2 thin films can be simply synthesized after removing the molecular templates by thermal annealing. Polyoxyethylene ether surfactant has a good solubility in water. When the concentration of the solution exceeds the critical micelle consistency (CMC), the molecular surfactant aggregates in the form of micelles, and disperses uniformly in the solution. During the gelation process, these micelles form the coagulation nucleus, and the network structure of gelatum will congregate around these micelles. With the post-formation thermal treatment, the molecular templates are removed due to their low decomposition temperature [14], as confirmed through FTIR measurement and DTA (Fig. 3) analysis. On the other hand, a process of significant surface modification is also needed. There are large amounts of non-associated –OH bonds on the pore surfaces of the as-deposited film. With volatilization of the solvent in the films, the pores shrink accordingly, and the distances among –OH bonds are reduced. The interaction between –OH bonds strengthens and results in the collapse of the pores in films. As a result of surface modification, a large amount of –OH bonds are replaced by $–CH_3$ bonds which are only weakly chemical active. The collapse of the pores, therefore, weakens and leaves a high pore density in the films. Besides the two aspects mentioned above, the effect of *n*-hexane is also undeniable. Based on the chemical properties of *n*-hexane, the washing process before the surface modification plays an important role for the efficiency of surface modification.

TG/DTA analysis was further carried out in a temperature range of 20 to 500 °C to detect the components

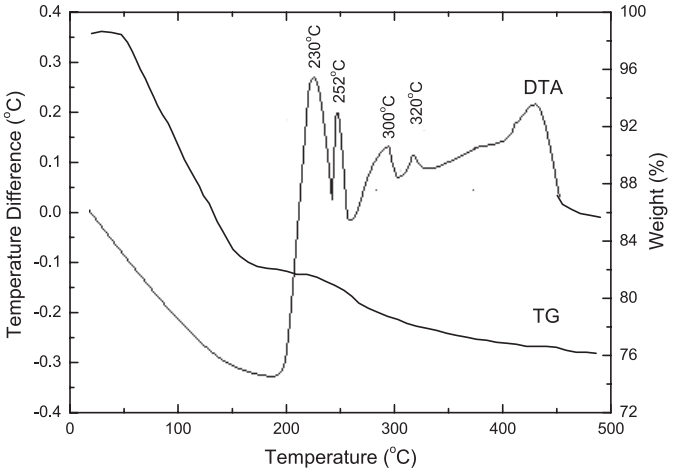

Fig. 3. TG/DTA curves of samples modified and dried gel monolith at 50 °C.

in the prepared films. The measured sample was SiO_2 gel monolith, which was synthesized by the same process as the modified film. As seen in Figure 3, the weight loss occurring at the temperature range of approximately 50 to 450 °C was related to the evaporation of solvent, water and organic composition. In the range of 50 to 200 °C, there was an obvious endothermic peak, which originated from the loss of solvent and water. The exothermic peaks in the range of 200 to 250 °C were attributed to the decomposition and pyrolytic loss of surfactant molecular templates and organic materials in the SiO_2 film. Besides the peaks, there were some other exothermic peaks around 300 °C. These peaks corresponded to the oxidation of $–CH_3$ bonds. The exothermic reactions remained active up to 450 °C, showing good correspondence with that of the FTIR spectra shown in Figure 2.

Based on the investigations above, we believe that the thermal treatment was necessary to obtain nanoporous SiO_2 films. Thermal annealing at 200 °C resulted in the decomposition of the templates and the formation of pores in the films. This can greatly decrease the k value of the nanoporous SiO_2 films. Regarding the fact that high temperature thermal treatments deteriorated the hydrophobicity of the films, and Cu low-k processing required a temperature up to at least 350 °C, our study has shown that $–CH_3$ bonds exist in the films even after thermal treatment at 450 °C for 2 h, as seen in Figure 2. Therefore, the thermal annealing only partially induces the oxidation of $–CH_3$ bonds of the films; the films still show good hydrophobicity after thermal treatment at 450 °C.

After removing the molecular templates through thermal annealing, we obtained nanoporous films with high porosity. However, our ultimate aim is to reduce the k value of the films so as to make them more useful in the future for ULSI technology. There are four kinds of models to predict the dielectric constant of the films from the porosity as shown in Figure 4. The two extreme cases are the parallel and the serial models, respectively, to predict

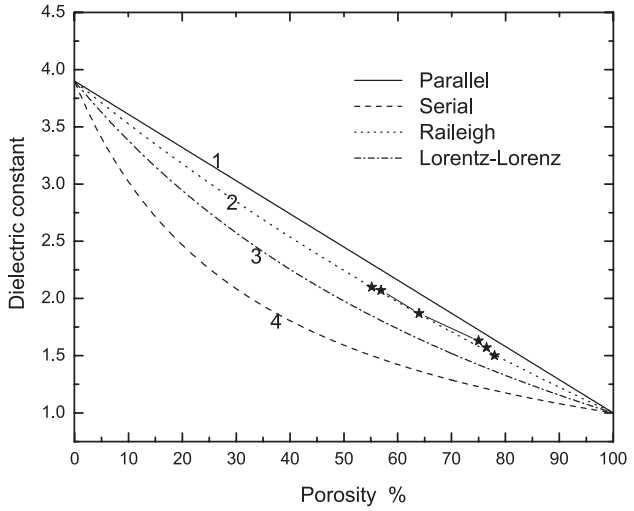

Fig. 4. The four kinds of model describing the dielectric constant as a function of the porosity.

the highest and lowest value of the dielectric constant,

$$k_{\text{Parallel}} = k_{\text{wall}} - (k_{\text{wall}} - k_{\text{pore}})P \tag{1}$$

$$\frac{1}{k_{\text{Serial}}} = \frac{1}{k_{\text{wall}}} - \left(\frac{1}{k_{\text{wall}}} - \frac{1}{k_{\text{pore}}}\right)P \tag{2}$$

where P is the porosity k_{wall} and k_{pore} are the relative dielectric constant of the wall dielectric medium and the pore, respectively. The other two models in this study include Rayleigh and Lorentz-Lorenz models. Our results (stars) were found to fit well to the Rayleigh model, which assumed a uniform distribution of spherical pores in a porous film, and can be expressed as,

$$k_{\text{Rayleigh}} = k_{\text{wall}}\left\{1 + \frac{3P(k_{\text{pore}} - k_{\text{wall}})}{2k_{\text{wall}} + k_{\text{pore}} - P(k_{\text{pore}} - k_{\text{wall}})}\right\}. \tag{3}$$

It is well known that the parallel model can well describe the dielectric constant of porous silica thin films that contain pores extending mostly from the bottom to the front surface. If the films have uniformly distributed pores with closed air gaps, the dielectric constant is better expressed by the serial model. Our experiment data are close to the upper limit of the parallel model due to high concentration of molecular templates. Very high concentration of template may result in the interpenetration of the pores, while too little content cannot support the network structure of the films, leading to the presence of big pores which also induce interpenetration of the structure. Therefore, in future work, we will investigate the effect of concentration of the molecular templates on the structural properties of the nanoporous films.

The actual microstructure of the films including the pore size and the porosity was observed by TEM. Figure 5 compares two TEM images of the modified nanoporous silica films under thermal annealing at 150 °C (Fig. 5a) and 450 °C (Fig. 5b), respectively. In comparison with that in Figure 5a, the surface morphology of the film in Figure 5b exhibits higher porosity. The distribution of pore size was much more uniform and the pore size was smaller (10–20 nm). The pore size observed by TEM was a little bigger than that of the BJH adsorption average pore width (9.8 nm) calculated by N_2 absorption/desorption data as shown in Figure 6. This result may be due to the presence of very small pore in the grains of the films, which results in the error in the relationship between the dielectric constant and the porosity presented in Figure 4. The thickness of the film showed no significant change according to the cross-sectional SEM morphology, as shown in Figure 7. From the results of ellipsometry, the thickness of the films was around 495 nm throughout, even after being thermally treated at 450 °C. This implies that the shrinkage (collapse) of the silica network did not occur after thermal treatment. Since surface modification can substitute the –OH in pore surface with $–CH_3$ bonds, the additional reaction between –OH bonds resulting from capillary force was prevented [12].

In order to have an accurate estimation of the distribution of pore size, we carried out N_2 adsorption/desorption measurements. As shown in Figure 6, the N_2 adsorption/desorption isotherms of the films by thermal treatment at different temperatures were investigated as a function of the relative partial pressure. The isotherm in films thermally treated at 150 °C was a typical behavior for microporous films, since it did not show a hysteresis loop. This means that the film was relatively compact, and only some micropores exist inside the film. By comparison, we could deduce that there may be many more mesopores in the film treated at 450 °C, due to the decomposition of the template material.

The dielectric constant, thickness and porosity of the prepared films through different kinds of thermal post-treatment are presented in Figure 8. The dielectric constant (k) and porosity (P) were determined from $C - V$ curves and the optical refractive index (n), respectively. The value of n was measured by ellipsometry, and the porosity was calculated using the relation [15], $P = 1 - \rho_{\text{f}}/\rho_{\text{s}}$ (where ρ_{f} was the film density having connection with optical refractive index, $\rho_{\text{f}} = (n-1)/0.209$, and ρ_{s} was the density of conventional SiO_2 films). The dielectric constant of the as-deposited film was determined to be 2.1. When the as-deposited film was processed under further post-treatment, i.e. surface modification and thermal treatment in N_2 atmosphere, the dielectric constant of the film reduced. With sufficient surface modification in TMCS/n-hexane solution and thermal treatment at 200 °C in air, a dielectric constant of 1.87 was obtained. The decrease of dielectric constant was attributed to the substitution of $–CH_3$ bonds for highly polarized –OH bonds and the pyrolytic decomposition of the organic component. During the thermal treatment, the N_2 atmosphere can limit the oxidation of $–CH_3$ bonds, and enhance the hydrophobicity of the film, giving a further decrease in k value. Thermal annealing at 450 °C in N_2 further reduced the dielectric constant to 1.5 from 1.87. The porosity of the film increased from 64% to 78%, implying that the decrease of dielectric constant also resulted from the increase of porosity at high temperature thermal treatment.

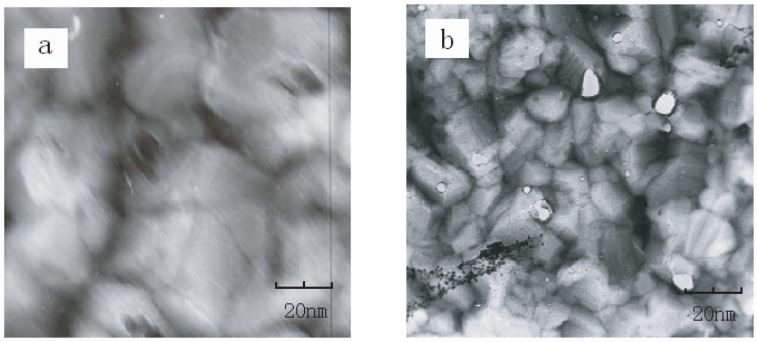

Fig. 5. TEM images of the samples that have been significantly modified in TMCS/*n*-hexane solution and thermally treated in N_2 atmosphere at (a) 150 °C and (b) 450 °C, respectively.

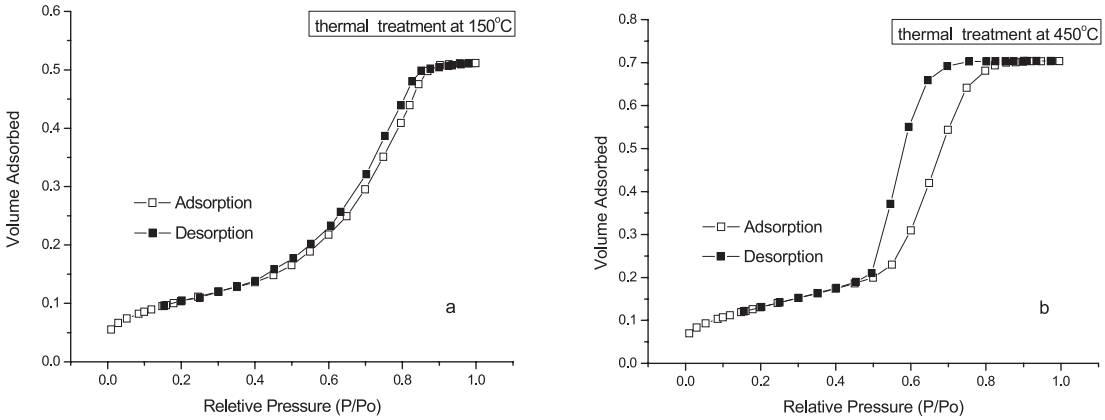

Fig. 6. N_2 adsorption/desorption isotherms for samples thermally treated at temperatures of (a) 150 °C; (b) 450 °C, respectively.

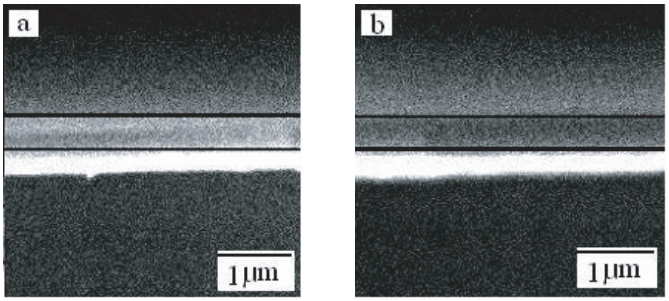

Fig. 7. SEM images of the samples that have been significantly modified in TMCS/*n*-hexane solution and thermally treated in N_2 atmosphere at (a) 150 °C and (b) 450 °C, respectively.

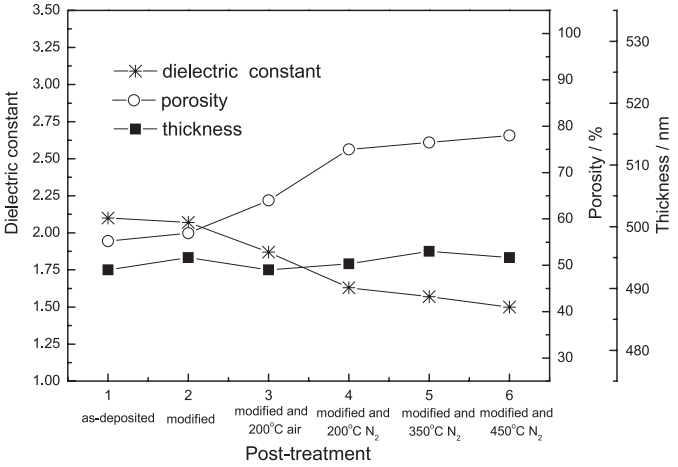

Fig. 8. The dielectric constant and porosity as a function of different post treatments.

4 Conclusion

In this study, nanoporous SiO_2 thin films with ultra-low k values have been synthesized using sol-gel method under assistance with molecular templates. During the post-treatments, *n*-hexane washing is found to play an important role in surface modification. FTIR analysis shows that the chemical bonds and bonding environment changed after surface modification and thermal annealing. The results are in line with DTA analysis. Furthermore, after thermal treatment at different temperatures (50–450 °C) in N_2 atmosphere, the structural properties of the films are improved. TEM images and N_2 adsorption/desorption isotherms indicate that the films have a relatively small pore size distribution (10–20 nm) and good network structure. The low dielectric constant of 1.5 as well as a porosity of 78% is obtained. The relationship between dielectric constant and porosity can be well explained by the Rayleigh model, which assumes a uniform distribution of spherical pores in a porous film.

The work was supported by grants no. 50272027 and 50402024 from the National Natural Science Foundation of China, and no. 3ZS041-A25-033 from the Province Science Foundation of Gansu.

References

1. O. Larlus, S. Mintova, V. Valtchev et al., Appl. Surf. Sci. **226**, 155 (2004)
2. M.E. Clarke, Introducing low-k dielectrics into Semiconductor Processing, Mykrolis, Applications notes, MAL123 (2003)
3. D.H. Wang et al., Solid State Technol. **10**, 101 (2001)
4. R.D. Miller, Science **286**, 4 (1999)
5. C.H. Ronald, H.-J. Lee, B.J. Bauer, Langmuir **20**, 416 (2004)
6. Y.Y. Jin, Kihong Kim, G.S. Lee, J. Vac. Sci. Technol. B **19**(1), 314 (2001)
7. C. Murray, C. Flannery, I. Streiter, et al., Microelectron. Eng. **60**, 133 (2002)
8. Z.B. Wang, A. Mitra, L. Huang, Y.S. Yan, Adv. Mater. **13**, 746 (2001)
9. S. Baskaran, et al., Adv. Mater. **12**, 291 (2000)
10. Z.W. He, C.M. Zhen, X.Q. Liu, et.al., Thin Solid Films **462–463**, 168 (2004)
11. C.J. Brinker, G.W. Scherer, Sol-Gel Sci., 581 (1990)
12. T.C. Chang, et al., Thin Solid Films **420**, 403 (2002)
13. G.M. Wu et al., Acta. Phys. Sin. **51**, 104 (2002)
14. C.M. Yang, A.T. Cho, F.-M. Pan, T.-G. Tsai, K.-J. Chao, Adv. Mater. **13**, 1099 (2001)
15. S.K. Gun, H.H. Sang, Thin Solid Films **460**, 190 (2004)